Evolution of Eukaryotic Ion Channels: Principles Underlying the Conversion of Ca2+-Selective to Na+-Selective Channels

ARTICLE *in* JOURNAL OF THE AMERICAN CHEMICAL SOCIETY · FEBRUARY 2014

Impact Factor: 12.11 · DOI: 10.1021/ja4121132 · Source: PubMed

2 AUTHORS:

Todor Dudev
Academia Sinica
45 PUBLICATIONS **1,664** CITATIONS
SEE PROFILE

Carmay Lim
Academia Sinica
144 PUBLICATIONS **4,082** CITATIONS
SEE PROFILE

PCCP

View Online / Journal Homepage
Dynamic Article Links

Cite this: DOI: 10.1039/c2cp00036a

www.rsc.org/pccp

PAPER

Why voltage-gated Ca^{2+} and bacterial Na^{+} channels with the same EEEE motif in their selectivity filters confer opposite metal selectivity

Todor Dudev*[a] and Carmay Lim*[ab]

Received 5th January 2012, Accepted 17th February 2012
DOI: 10.1039/c2cp00036a

Voltage-gated sodium (Na_v) and calcium (Ca_v) channels, which play essential biological roles, are characterized by their ability to discriminate the "native" ion from other competing cations. Surprisingly, Na^+-selective bacterial Na_v and high voltage-activated Ca^{2+}-selective Ca_v channels both exhibit selectivity filters (the narrowest part of the open pore) lined by four Glu residues that interact specifically with the permeating ions. This raises the intriguing question why selectivity filters with the same EEEE motif are Na^+-selective in Na_v channels but Ca^{2+}-selective in Ca_v channels. We show that the different degree of metal hydration inside the pore, which is related to the pore size and rigidity, can account for the opposite ion selectivity in Na_v and Ca_v channels with identical EEEE selectivity filters. The results are consistent with experimental estimates of the metal hydration structure in Na_v and Ca_v channels with the EEEE motif. They suggest that the protein matrix, which can enhance or attenuate ion–protein interactions relative to ion–solvent interactions by controlling the pore's solvent accessibility, size/rigidity, and charge state, is a key determinant of Ca^{2+} *vs.* Na^+ selectivity in EEEE selectivity filters.

I. Introduction

Voltage-gated sodium (Na_v), potassium (K_v), and calcium (Ca_v) channels are indispensable integral components of living cells and play a key role in regulating the cardiac, skeletal and smooth muscle contraction, hormone secretion, taste and pain sensation, and signal transduction.[1,2] Hence, their malfunctions often lead to channelopathies of the heart, skeletal muscle, and brain such as arrhythmia, ataxia, epilepsy, erythromelalgia, hypertension, migraine, neuromyotonia, periodic paralysis, and Timothy syndrome.[3] The three types of voltage-gated ion channels are characterized by their remarkable metal selectivity, allowing them to discriminate between the "native" ion and other competing metal cations from the cellular/extracellular milieu.

The selectivity of voltage-gated ion channels is controlled by their selectivity filters—the narrowest part of the open pore lined with residues that interact specifically with the passing ions. In the absence of the metal-bound Na_v and Ca_v channel structures, the selectivity filter residues have been determined mainly from mutagenesis studies. In vertebrate Na_v channels, Asp, Glu, Lys, and Ala residues from the channel's four different domains line an asymmetric selectivity filter (DEKA locus),[4–10] whereas in the bacterial counterparts, four Glu residues donated by the channel's four identical subunits comprise a symmetrical selectivity filter (EEEE locus).[11,12] In line with mutagenesis studies,[12] the 2.7 Å X-ray structure of a bacterial Na_v channel captured in a closed-pore, metal-free conformation reveals four Glu side chains lining a short, water-filled selectivity filter.[11] Remarkably, the high voltage-activated Ca_v channel selectivity filter also comprises four Glu residues that have been found to be key determinants of ion selectivity from mutagenesis studies.[13–20]

Although 3D structures of metal-bound Na_v and high voltage-activated Ca_v channels with EEEE selectivity filters have not yet been solved, alignment of their selectivity filter sequences shows that the four Na_v channel Glu residues align with the four Ca_v channel Glu residues and the pore architecture of the Ca_v channel is highly similar to that observed in the bacterial Na_v channel crystal structure.[11] However, the high voltage-activated Ca_v channels are highly selective for Ca^{2+} over Na^+ by a ratio of $\sim$1000 : 1,[1,2] whereas the bacterial Na_v channels exhibit a Na^+ : Ca^{2+} permeability ratio of $\sim$15 and a Na^+ : K^+ permeability ratio of 170.[12] The observed selectivity for Na^+ over Ca^{2+} in EEEE selectivity filters of bacterial Na_v channels is quite puzzling since high voltage-activated Ca_v channels with the same EEEE motif are Ca^{2+}-selective.

Herein, we elucidate the determinants of Na^+ *vs.* Ca^{2+} selectivity in filters with the EEEE motif by computing the free energy for replacing Ca^{2+} bound directly to 0, 2, 3, and 4 Glu

[a] *Institute of Biomedical Sciences, Academia Sinica, Taipei 115, Taiwan. E-mail: todor@ibms.sinica.edu.tw, carmay@gate.sinica.edu.tw*
[b] *Department of Chemistry, National Tsing Hua University, Hsinchu 300, Taiwan*

side chains in model EEEE selectivity filters (denoted by $[Ca(H_2O)_n\text{-E4filter}]^{-2}$; $n = 0, 1, 2, 4$) with a nearby Na^+:

$$[Na(H_2O)_6]^+ + [Ca(H_2O)_n\text{-E4filter}]^{-2} + H_2O \rightarrow [Na(H_2O)_n\text{-E4filter}]^{-3} + [Ca(H_2O)_7]^{2+} \quad (1)$$

The metal cation and its ligands were treated explicitly using density functional theory calculations to account for electronic effects such as polarization of the participating entities and charge transfer from the ligands to the metal cation, which cannot be accurately treated using classical force fields in molecular dynamics simulations. Since the ion channel selectivity filter and its immediate surroundings are not in a bulk water environment,[21,22] the reactions were modeled in an environment represented by a continuum dielectric x varying from 4 (buried, solvent-inaccessible binding site) to 30 (solvent-accessible binding site), reflecting an increasingly solvent-exposed pore.[22,23] The ion exchange free energy for eqn (1), ΔG^x, is given by:

$$\Delta G^x = \Delta G^1 + \Delta G_{solv}{}^x([Na(H_2O)_n\text{-E4filter}]) + \Delta G_{solv}{}^x([Ca(H_2O)_7]) - \Delta G_{solv}{}^x([Ca(H_2O)_n\text{-E4filter}]) - \Delta G_{solv}{}^x([Na(H_2O)_6]) - \Delta G_{solv}{}^x(H_2O) \quad (2)$$

ΔG^1, the gas-phase free energy for eqn (1), and $\Delta G_{solv}{}^x$, the free energy for transferring a molecule in the gas phase to a medium characterized by dielectric constant x, were computed as described in the Methods section. Positive ΔG^x values imply a Ca^{2+}-selective EEEE filter, whereas negative ΔG^x numbers imply a Na^+-selective one.

II. Methods

A. Models used

Models of tetrameric selectivity filters with an EEEE locus (see Fig. 1) were built using GaussView version 3.09,[24] following the guidelines from our previous works.[23,25] Compared to earlier "toy" models[26] and other simplified structures[21,27–29] used in studying metal selectivity in ion channels, our augmented models bear closer resemblance to the channel's selectivity filter as (1) the ring mimics the oligomeric state and overall symmetry/asymmetry of the ion channel pore and prevents the metal-binding groups from drifting away during geometry optimization; (2) the metal-ligating groups and their connection to the ring are flexible enough to allow them to optimize their positions upon metal binding; and (3) the shape and C–H bond orientations of the ring do not obstruct the pore lumen. The Glu residues were modeled as deprotonated in line with the results from mutagenesis experiments on Ca_v channels—mutating any of these Glu residues to a neutral one weakens Ca^{2+} binding by up to 50-fold.[15,16] The Na^+ and Ca^{2+} hydrates were modeled as $[Na(H_2O)_6]^+$ and $[Ca(H_2O)_7]^{2+}$, respectively, in accord with experimental observations.[30,31]

B. Gas-phase free energy calculations

Among several combinations of different *ab initio* methods/density functionals and basis sets, the B3-LYP/6-31+G(3d,p) has been shown to be the most efficient in reproducing dipole moments of the metal–ligands and metal–ligand distances in crown-ether complexes (resembling ion channel pores) to within experimental error[23,25] (see Table 1). Hence, it was used to optimize the geometry of each metal complex and to evaluate the vibrational frequencies using the Gaussian 09 program.[32] No imaginary frequency was found in any of the complexes. The frequencies were scaled by an empirical factor of 0.9613[33] and used to compute the thermal energies and

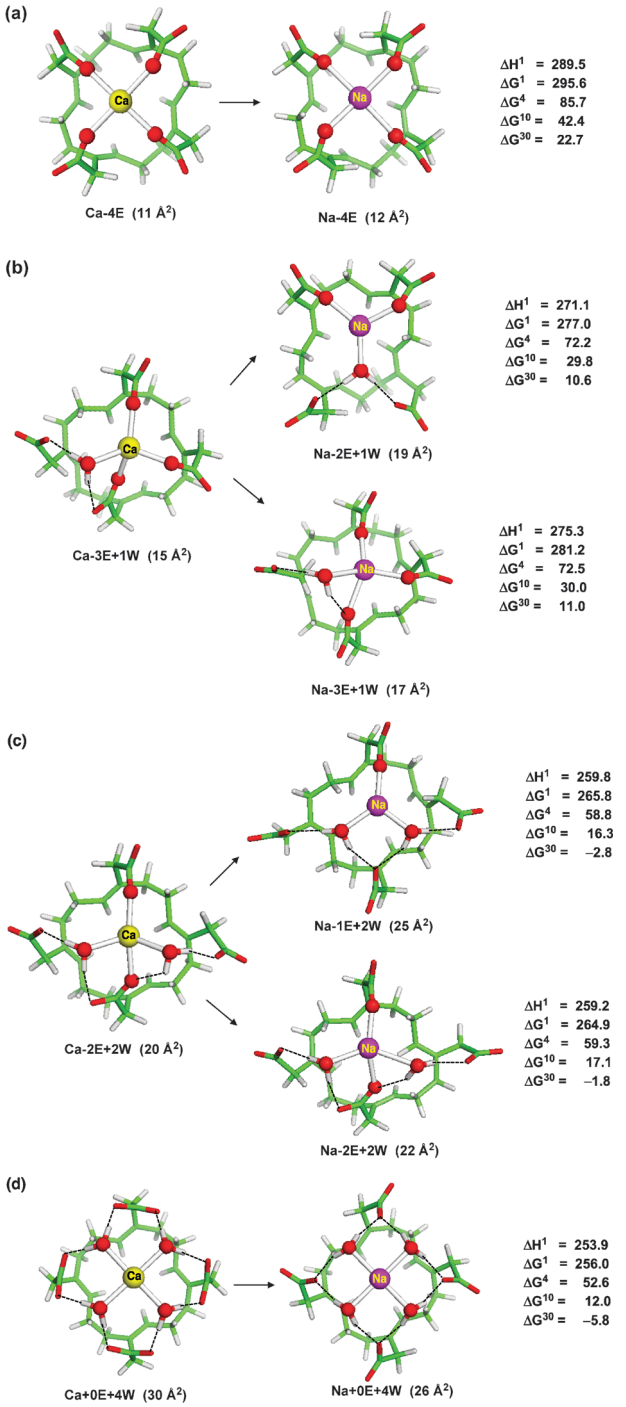

Fig. 1 Dependence of the enthalpies and free energies (in kcal mol^{-1}) for the $Na^+ \rightarrow Ca^{2+}$ exchange in eqn (1) on the number of metal-bound water molecules. The metal cation is bound to (a) 0, (b) 1, (c) 2, and (d) 4 water molecules inside the EEEE selectivity filter. Fully optimized B3LYP/6-31+G(3d,p) structures are shown with C in green, H in grey, O in red, Ca^{2+} in yellow, Na^+ in magenta. The aperture area of the pore, computed as shown in Fig. 3, is in parentheses.

Table 1 Comparison between computed and experimental gas-phase dipole moment μ of H_2O, average metal–oxygen bond distances in metal-bound crown ethers, hydration free energies, ΔG_{solv}^{80}, of metal cations and ligands, and free energies of metal exchange, ΔG_{ex}^{80}, in nitrilotriacetic acid (NTA) complexes

Compound/reaction	Parameter	Calculated	Experimental
H_2O	μ/D	1.88	1.85 ± 0.02^a
$[Na(18\text{-crown-}6)]^+$	Na–O/Å	2.75	2.77 ± 0.07^b
$[Ca(H_2O)_3(18\text{-crown-}6)]^{2+}$	Ca–O/Å	2.66	2.60 ± 0.07^c
Na^+	ΔG_{solv}^{80}/kcal mol^{-1}	−98.7	-98.3^d
Ca^{2+}		−381.1	-380.8^d
H_2O		−6.7	-6.3^e
CH_3COO^-		−82.3	-82.2^f
$[Na(H_2O)_6]^+ + H_2O + [Ca(H_2O)_2(NTA)]^- \rightarrow [Na(H_2O)_2(NTA)]^{2-} + [Ca(H_2O)_7]^{2+}$	ΔG_{ex}^{80}/kcal mol^{-1}	6.7	7.1^g

[a] From Lide, 2006.[43] [b] From Cambridge Structure Database analysis (Dudev and Lim, 2009[25]). [c] From Cambridge Structure Database analysis (this work); the average bond distance between Ca^{2+} and crown-ether oxygen atoms is given. [d] From Friedman and Krishnan, 1973.[44] [e] From Ben-Naim and Marcus, 1984.[45f] From Lim *et al.*, 1991.[46g] Calculated from the experimental stability constants of the respective metal complexes from Smith and Martell;[42] NTA binds in a tetradentate fashion (including central N atom) to the metal.

entropies. The differences in the electronic energy (ΔE_{el}), thermal energies (ΔE_{th}), work term (ΔPV) and entropies (ΔS) between the products and reactants in eqn (1) were used to calculate the gas-phase free energy for eqn (1), ΔG^1, at $T = 298.15$ K according to:

$$\Delta G^1 = \Delta E_{el} + \Delta E_{th} + \Delta PV - T\Delta S \quad (3)$$

C. Solution free energy calculations

The ΔG_{solv}^{x} energies in eqn (2) were estimated by solving Poisson's equation using the MEAD program[34] as described in our previous work.[25] Natural Bond Orbital (NBO) atomic charges, which are known to be numerically quite stable with respect to basis set changes,[35] were used in the calculations. The effective solute radii were obtained by adjusting the CHARMM version 22[36] van der Waals radii to reproduce the experimental hydration free energies of Na^+, Ca^{2+}, and model ligand molecules to within 1 kcal mol^{-1} (see Table 1). Poisson's equation was solved for $x = 4$, 10, and 30 to mimic binding sites with increasing solvent exposure. Since the metal ion exchange was modeled to occur in the vicinity of the selectivity filter, the dielectric environment was assumed to be uniform for the participating entities in eqn (1); any change in the dielectric environment would not be expected to be significant, and would thus not alter the trends in the free energy changes reported herein.

D. Solution free energy calibration

The above calculations do not aim at reproducing the absolute metal exchange free energies in Na_v and Ca_v channels with the EEEE motif. Rather, they aim to yield reliable trends in the free energy changes with varying numbers of carboxylates and water molecules bound to the metal cation. Notably, our previous calculations have yielded trends in the free energy changes that are in line with experimental observations.[23,25,37–41] To further ascertain the accuracy of the ion exchange free energy calculations in revealing reliable trends, we computed ΔG^{80} for replacing dihydrated Ca^{2+} bound to nitrilotriacetic acid (NTA) with Na^+ in aqueous solution; *i.e.*, $[Na(H_2O)_6]^+ + H_2O + [Ca(H_2O)_2(NTA)]^- \rightarrow [Na(H_2O)_2(NTA)]^{2-} + [Ca(H_2O)_7]^{2+}$. The resulting ΔG^{80} of 6.7 kcal mol^{-1} is in close agreement with the respective experimental value of 7.1 kcal mol^{-1}.[42]

III. Results and discussion

Fig. 1 shows the computed free energies for replacing Ca^{2+} bound directly to 4, 3, 2 and 0 Glu side chains retaining 0, 1, 2, and 4 water molecules, respectively, in model EEEE selectivity filters. As the reactions depicted in Fig. 1 involve the exchange of Ca^{2+} for Na^+ in relatively large model EEEE selectivity filters, systematic errors in the computed gas-phase and solvation free energies of the reactants are likely to partially cancel those of the respective products (see eqn (1)). Furthermore, errors in the gas-phase energies have been minimized by choosing the method/basis set that can yield experimental dipole moments of the metal–ligands and metal–ligand distances, whereas errors in the solvation free energies have been accounted by calibrating the atomic radii to reproduce the experimental hydration free energies of the metal cations and ligands (see Methods and Table 1). While interpreting the results, we focus on how the free energy changes upon increasing the number of metal bound water molecules and solvent exposure of the pore.

A. Opposing effects of ion–protein and ion–water interactions

The computed gas-phase ΔH^1 enthalpies and ΔG^1 free energies in Fig. 1 show that the reactions are enthalpy driven in the gas phase, as ΔH^1 accounts for 98–99% of ΔG^1. Ion–protein electrostatic interactions strongly favor divalent Ca^{2+} over monovalent Na^+ in an EEEE selectivity filter, resulting in very unfavorable $Na^+ \rightarrow Ca^{2+}$ free energies in the gas phase (large positive $\Delta G^1 = 256$–296 kcal mol^{-1}). On the other hand, ion–solvent electrostatic interactions favor Na^+ over Ca^{2+} due mainly to the stronger solvation of the highly charged products compared to the reactants in eqn (1): the trianionic Na complex is better solvated than the respective dianionic Ca complex, while the strong solvation of the outgoing Ca^{2+} compensates for the desolvation penalty of the incoming Na^+. This effect is enhanced (favoring Na^+) with increasing solvent exposure of the pore (ΔG^x decreases with increasing dielectric constant x).

B. Increasing metal hydration favors Na^+ over Ca^{2+} in a water-filled EEEE selectivity filter

Pores where the passing cation is totally dehydrated are selective for Ca^{2+} over Na^+, even if the pore is relatively

solvent-exposed (Fig. 1a, large positive ΔG^x, x = 4–30). Larger pores that allow the cation to indirectly bind a Glu side chain *via* a water molecule are also Ca^{2+}-selective, even if the Na^+ coordination number changes[23] (Fig. 1b, positive ΔG^x for reaction yielding tricoordinated **Na-2E + 1W** and tetracoordinated **Na-3E + 1W**). Relative to the gas-phase ΔG^1 for the fully dehydrated **Ca-4E** (296 kcal mol^{-1}), ΔG^1 for monohydrated **Ca-3E + 1W** (277–281 kcal mol^{-1}) is smaller due to the loss of a direct metal–carboxylate contact, resulting in longer metal–O distances, which disfavors Ca^{2+} binding more than Na^+ binding: as the distance between the metal and a carboxylate oxygen (r_{M-O}) is stretched from its equilibrium distance, the electronic energy of the Ca^{2+}-complex increases much more rapidly than that of the respective Na^+-complex (see Fig. 2). Consequently, further increase in the number of water-mediated metal–carboxylate interactions additionally lowers the respective ΔG^1 values, resulting in decreased Ca^{2+} selectivity of the pore (Fig. 1c and d). Notably, solvent-exposed EEEE selectivity filters that can accommodate 2 to 4 metal-bound water molecules become selective for Na^+ over Ca^{2+}: ΔG^{30} = −2.8 kcal mol^{-1} for dihydrated cations (Fig. 1c) and −5.8 kcal mol^{-1} for tetrahydrated cations (Fig. 1d).

C. Metal hydration, pore size, and ion selectivity

The degree of metal hydration inside the pore is correlated with the pore size, which was estimated as the area formed by the four carboxylate oxygen atoms facing the pore lumen, as illustrated in Fig. 3 for the **Ca-4E** selectivity filter in Fig. 1a. As the number of water-mediated Ca^{2+}–carboxylate interactions increases from 0, 1, 2, to 4, the maximal distance between two carboxylate oxygen atoms facing the pore lumen increases from 3.25, 4.69, 5.34, to 5.76 Å, while the pore aperture area increases from 11, 15, 20, to 30 Å^2, respectively (see Fig. 1). Thus, a narrow, rigid EEEE filter that excludes solvent with all

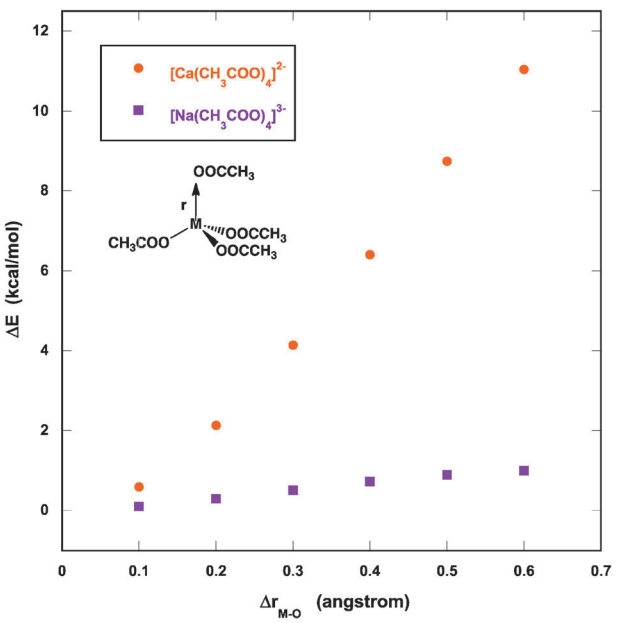

Fig. 2 Plot of the changes in electronic energy $\Delta E = E_{distorted} - E_{opt}$ of the $[M(CH_3COO)_4]^{+/2+}$ (M = Na or Ca) metal complexes as a function of M–O bond stretching.

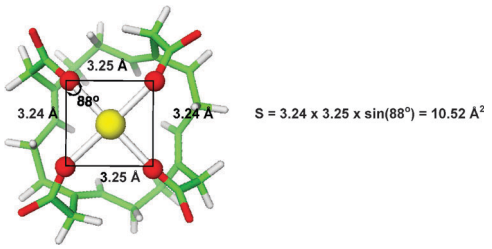

Fig. 3 Calculation of the pore aperture area in a model EEEE selectivity filter containing fully dehydrated Ca^{2+} (Fig. 1a). The aperture areas of the other complexes in Fig. 1 were computed in a similar way.

four carboxylates binding directly to a fully dehydrated ion would maximize Ca^{2+}/Na^+ selectivity (Fig. 1a). Conversely, a wide, rigid EEEE filter that allows solvent with two or more carboxylates binding indirectly to a partially dehydrated ion *via* water bridges would enhance Na^+/Ca^{2+} selectivity (Fig. 1c and d).

D. Comparison with experiment: mapping of the observed metal hydration structure in an EEEE selectivity filter to the computed free energies

Experimental estimates of the metal hydration structure in Na_v and Ca_v channels with the EEEE motif can be correlated with the structures and free energies in Fig. 1. In high voltage-activated Ca_v channels, the EEEE selectivity filter has an estimated pore diameter of 6.0[47]–6.2[48] Å (or an aperture area of 18.0–19.2 Å^2) from studies on the permeation of large organic cations—such an orifice has been suggested to fit Ca^{2+} with a bound water.[47] Indeed, as shown in Fig. 1b, a pore (with an aperture area of 15–19 Å^2) fitting a monohydrated cation is selective for Ca^{2+} over Na^+ (positive ΔG^x). This is mainly due to the more favorable interactions of the Glu carboxylates with Ca^{2+} than with Na^+, yielding a free energy gain, which can overcome the greater dehydration penalty of Ca^{2+} relative to that of Na^+ as well as the poorer solvation of the dianionic Ca complex in the EEEE selectivity filter compared to the respective trianionic Na complex. In comparison to such a pore, a pore fitting a fully dehydrated cation would exhibit even greater Ca^{2+}/Na^+ selectivity (Fig. 1a); however, the stronger interactions between all 4 Glu carboxylates and Ca^{2+} might slow down ion conductance.

The EEEE selectivity filter of a bacterial Na_v channel is significantly wider than that of high voltage-activated Ca_v channels or the DEKA locus of vertebrate Na_v channels: its crystal structure shows a wide, water-lined pore with an aperture area of ~21 Å^2 that has been hypothesized to accommodate a metal cation, retaining two water molecules in the plane of the selectivity ring.[11] Indeed, as shown in Fig. 1c, a water-containing pore (with an aperture area of 20–25 Å^2) fitting a dihydrated cation is selective for Na^+ over Ca^{2+} (negative ΔG^x, $x \geq 30$). Compared to a monohydrated cation in an EEEE selectivity filter, ion–carboxylate interactions still favor Ca^{2+} over Na^+, but to a lesser extent due to fewer direct ion–carboxylate interactions (ΔG^1 for **Ca-2E + 2W** is less than ΔG^1 for **Ca-3E + 1W**); thus the ion–carboxylate interactions cannot outweigh the ion–solvent interactions, which favor Na^+

over Ca^{2+}. Interestingly, the magnitude of ΔG^{30} for the dihydrated Ca^{2+} in Fig. 1c (-2.8 kcal mol^{-1}) is smaller and opposite in sign to that for the respective monohydrated Ca^{2+} in Fig. 1b (11 kcal mol^{-1}), indicating that Na^+/Ca^{2+} selectivity is not as strong as Ca^{2+}/Na^+ selectivity. This is consistent with the much smaller permeability ratio of Na^+ to Ca^{2+} ($\sim$15) in bacterial Na_v channels compared to that of Ca^{2+} to Na^+ ($\sim$1000) in high voltage-activated Ca_v channels (see Introduction).

The EEEE selectivity filter of the high voltage-activated Ca_v or bacterial Na_v channel has to be relatively rigid to maintain a given pore size. There is some evidence indicating that the selectivity filters in Na_v channels are relatively rigid. The recent crystal structure of a bacterial Na_v channel shows that both backbone and side chain oxygen atoms of the Glu residues lining the EEEE selectivity filter form hydrogen bonds with neighboring backbone amides,[11] rigidifying the pore and constraining its size. The DEKA selectivity filter of vertebrate Na_v channels is also stiff due to hydrogen bonds formed by the Lys side chain with the adjacent carboxylate and Ala carbonyl oxygen.[9,23,49–51]

IV. Conclusions

The above results indicate that a key determinant of Ca^{2+} *vs.* Na^+ selectivity in an EEEE selectivity filter lies in the protein matrix, which can enhance or attenuate ion–protein interactions relative to ion–solvent interactions by controlling the pore's solvent accessibility, size/rigidity, and Glu protonation state. The protein environment can enhance ion–protein interactions relative to ion–solvent interactions in an EEEE selectivity filter by limiting solvent access, restricting the pore to fit only dehydrated or monohydrated Ca^{2+}, and favoring deprotonation of all four Glu ligands; in this case, ion–protein electrostatic interactions dictate ion selectivity, favoring Ca^{2+} over Na^+. Conversely, the protein environment can enhance ion–solvent interactions relative to ion–protein interactions in an EEEE selectivity filter by allowing water inside the pore and enlarging the pore to accommodate two or more metal-bound water molecules or enabling two or more Glu residues lining the pore lumen to be protonated; in this case, solvation effects dictate ion selectivity, favoring Na^+ over Ca^{2+}.

This work has thus revealed a plausible physical basis for the opposite ion selectivity in bacterial Na_v and high voltage-activated Ca_v channels with the EEEE motif by mapping the experimentally observed metal hydration structure in these two types of channels to the respective computed metal exchange free energies: EEEE selectivity filters that bind fully dehydrated or monohydrated cations would be highly selective for Ca^{2+} over Na^+, whereas those with larger, water-filled pores that bind indirectly to cations *via* two or more water molecules would confer moderate Na^+/Ca^{2+} selectivity. Thus, subtle changes in the metal hydration structure can tilt the balance between ion–protein and ion–solvent interactions in favor of Na^+ or Ca^{2+}.

Acknowledgements

We thank Prof. James Wang and Prof. Tse Wen Chang for reading this work and helpful comments. This work was supported by Academia Sinica and NSC contract no. NSC 95-2113-M-001-001.

References

1 B. Hille, *Ionic channels of excitable membranes*, Sinauer Associates, Sunderland, MA, 2001.
2 J. E. Hall, *Guyton and Hall Textbook of Medical Physiology with Student Consult Online Access*, Elsevier Saunders, Philadelphia, 2011.
3 R. S. Kass, *J. Clin. Invest.*, 2005, **115**, 1986–1989.
4 M. Noda, H. Suzuki, S. Numa and W. Stuhmer, *FEBS Lett.*, 1989, **259**, 213–216.
5 H. Terlau, S. H. Heinemann, W. Stuhmer, M. Pusch, F. Conti, K. Imoto and S. Numa, *FEBS Lett.*, 1991, **293**, 93–96.
6 M. Pusch, M. Noda, W. Stuhmer, S. Numa and F. Conti, *Eur. Biophys. J.*, 1991, **20**, 127–133.
7 S. H. Heinemann, H. Terlau, W. Stuhmer, K. Imoto and S. Numa, *Nature*, 1992, **356**, 441–443.
8 P. H. Backx, D. T. Yue, J. H. Lawrence, E. Marban and G. F. Tomaselli, *Science*, 1992, **257**, 248–251.
9 I. Favre, E. Moczydlowski and L. Schild, *Biophys. J.*, 1996, **71**, 3110–3125.
10 M.-T. Perez-Garcia, N. Chiamvimonvat, E. Marban and G. F. Tomaselli, *Proc. Natl. Acad. Sci. U. S. A.*, 1996, **93**, 300–304.
11 J. Payandeh, T. Scheuer, N. Zheng and W. A. Catterall, *Nature*, 2011, **475**, 353–359.
12 L. Yue, B. Navarro, D. Ren, A. Ramos and D. E. Clapham, *J. Gen. Physiol.*, 2002, **120**, 845–853.
13 M. S. Kim, T. Morii, L. X. Sun, K. Imoto and Y. Mori, *FEBS Lett.*, 1993, **318**, 145–148.
14 S. Tang, G. Mikala, A. Bahinski, A. Yatani, G. Varadi and A. Schwartz, *J. Biol. Chem.*, 1993, **268**, 13026–13029.
15 J. Yang, P. T. Ellinor, W. A. Sather, J. F. Zhang and R. W. Tsien, *Nature*, 1993, **366**, 158–161.
16 P. T. Ellinor, J. Yang, W. A. Sather and Z. J. F. R. W. Tsien, *Neuron*, 1995, **15**, 1121–1132.
17 L. Parent and M. Gopalakrishnan, *Biophys. J.*, 1995, **69**, 1801–1813.
18 S. E. Koch, I. Bodi, A. Schwartz and G. Varadi, *J. Biol. Chem.*, 2000, **275**, 34493–34500.
19 X. S. Wu, H. D. Edwards and W. A. Sather, *J. Biol. Chem.*, 2000, **275**, 31778–31785.
20 S. M. Cibulski and W. A. Sather, *J. Gen. Physiol.*, 2000, **116**, 349–362.
21 S. Varma and S. B. Rempe, *Biophys. J.*, 2007, **93**, 1093–1099.
22 S. Varma, D. Sabo and S. B. Rempe, *J. Mol. Biol.*, 2008, **376**, 13–22.
23 T. Dudev and C. Lim, *J. Am. Chem. Soc.*, 2010, **132**, 2321–2332.
24 Gaussian, Pittsburgh, PA 15106, USA, 2000–2003.
25 T. Dudev and C. Lim, *J. Am. Chem. Soc.*, 2009, **131**, 8092–8101.
26 S. Y. Noskov, S. Berneche and B. Roux, *Nature*, 2004, **431**, 830–834.
27 D. Asthagiri, L. R. Pratt and M. E. Paulaitis, *J. Chem. Phys.*, 2006, **125**, 24701.
28 D. L. Bostick and C. L. Brooks III, *Proc. Natl. Acad. Sci. U. S. A.*, 2007, **104**, 9260–9265.
29 M. Thomas, D. Jayatilaka and B. Corry, *Biophys. J.*, 2007, **93**, 2635–2643.
30 Y. Marcus, *Chem. Rev.*, 1988, **88**, 1475–1498.
31 M. Dudev, J. Wang, T. Dudev and C. Lim, *J. Phys. Chem. B*, 2006, **110**, 1889–1895.
32 M. J. Frisch, G. W. Trucks, H. B. Schlegel, G. E. Scuseria, M. A. Robb, J. R. Cheeseman, G. Scalmani, V. Barone, B. Mennucci, G. A. Petersson, H. Nakatsuji, M. Caricato, X. Li, H. P. Hratchian, A. F. Izmaylov, J. Bloino, G. Zheng, J. L. Sonnenberg, M. Hada, M. Ehara, K. Toyota, R. Fukuda, J. Hasegawa, M. Ishida, T. Nakajima, Y. Honda, O. Kitao, H. Nakai, T. Vreven, J. A. Montgomery, Jr., J. E. Peralta, F. Ogliaro, M. Bearpark, J. J. Heyd, E. Brothers, K. N. Kudin, V. N. Staroverov, R. Kobayashi, J. Normand, K. Raghavachari, A. Rendell, J. C. Burant, S. S. Iyengar, J. Tomasi, M. Cossi, N. Rega, J. M. Millam, M. Klene, J. E. Knox, J. B. Cross, V. Bakken, C. Adamo, J. Jaramillo, R. Gomperts, R. E. Stratmann, O. Yazyev, A. J. Austin, R. Cammi, C. Pomelli, J. W. Ochterski, R. L. Martin, K. Morokuma, V. G. Zakrzewski, G. A. Voth, P. Salvador, J. J. Dannenberg, S. Dapprich, A. D. Daniels, O. Farkas, J. B. Foresman, J. V. Ortiz, J. Cioslowski and D. J. Fox, Gaussian, Inc, Wallingford CT, 2009.

33 M. W. Wong, *Chem. Phys. Lett*., 1996, **256**, 391–399.
34 D. Bashford, in *Scientific Computing in Object-Oriented Parallel Environments*, ed. Y. Ishikawa, R. R. Oldehoeft, V. W. Reynders and M. Tholburn, Springer, Berlin, 1997, vol. 1343, pp. 233–240.
35 A. E. Reed, L. A. Curtiss and F. Weinhold, *Chem. Rev*., 1988, **88**, 899–926.
36 B. R. Brooks, R. E. Bruccoleri, B. D. Olafson, D. J. States, S. Swaminathan and M. Karplus, *J. Comput. Chem*., 1983, **4**, 187–217.
37 T. Dudev and C. Lim, *J. Phys. Chem. B*, 2001, **105**, 4446–4452.
38 C. S. Babu, T. Dudev, R. Casareno, J. A. Cowan and C. Lim, *J. Am. Chem. Soc*., 2003, **125**, 9318–9328.
39 T. Dudev and C. Lim, *J. Am. Chem. Soc*., 2004, **126**, 10296–10305.
40 T. Dudev, L.-Y. Chang and C. Lim, *J. Am. Chem. Soc*., 2005, **127**, 4091–4103.
41 T. Dudev and C. Lim, *J. Am. Chem. Soc*., 2011, **133**, 9506–9515.
42 R. M. Smith and A. E. Martell, *Sci. Total Environ*., 1987, **64**, 125–147.
43 *Handbook of Chemistry and Physics*, ed. D. R. Lide, CRC Press, Boca Raton, 2006.
44 H. L. Friedman and C. V. Krishnan, in *Water: a comprehensive treatise*, ed. F. Franks, Plenum Press, New York, 1973, vol. 3, pp. 1–118.
45 A. Ben-Naim and Y. Marcus, *J. Chem. Phys*., 1984, **81**, 2016–2027.
46 C. Lim, D. Bashford and M. Karplus, *J. Phys. Chem*., 1991, **95**, 5610–5620.
47 E. W. McCleskey and W. Almers, *Proc. Natl. Acad. Sci. U. S. A*., 1985, **82**, 7149–7153.
48 M. Cataldi, E. Perez-Reyes and R. W. Tsien, *J. Biol. Chem*., 2002, **277**, 45969–45976.
49 Y. M. Sun, I. Favre, L. Schild and E. Moczydlowski, *J. Gen. Physiol*., 1997, **118**, 693–715.
50 K. Hilber, W. Sandtner, T. Zarrabi, E. Zebedin, O. Kudlacek, H. A. Fozzard and H. Todt, *Biochemistry*, 2005, **44**, 13874–13882.
51 D. Boda, W. Nonner, M. Valisko, D. Henderson, B. Eisenberg and D. Gillespie, *Biophys. J*., 2007, **93**, 1960–1980.